

Crossing phantom divide in $f(Q)$ gravity

Simran Arora^{1,*} and P.K. Sahoo^{1,†}

¹*Department of Mathematics, Birla Institute of Technology and Science-Pilani,
Hyderabad Campus, Hyderabad-500078, India.*

We investigate the possibility of crossing a phantom divide line in the extension of symmetric teleparallel gravity or the $f(Q)$ gravity, where Q is the non-metricity. We study the cosmic evolution of the effective equation of state parameter for dark energy considering exponential, logarithmic, and combined $f(Q)$ theories. Moreover, the exponential model behaves like the Λ CDM at high redshifts before deviating to $\omega_{eff} < -1$ or $\omega_{eff} > -1$, respectively, depending on the value of model parameter. It also approaches a de-sitter phase asymptotically. However, the crossing of the phantom divide line, i.e., $\omega = -1$, is realized in the combined $f(Q)$ theory. Furthermore, statefinder diagnostics are studied in order to differentiate between several dark energy models. To ensure the three model's stability, we employ the stability analysis using linear perturbations. We demonstrate how to reassemble $f(Q)$ via a numerical inversion approach based on existing observational constraints on cosmographic parameters and the potential of bridging the phantom divide in the resulting model. It explicitly demonstrates that future crossings of the phantom dividing line are a generic feature of feasible $f(Q)$ gravity models.

I. INTRODUCTION

The primary purpose of current and future cosmological investigations is to learn more about the true nature of cosmic acceleration by subjecting the conventional cosmological model Λ CDM (Λ cold dark matter) to the test as well as variations from it [1–4]. Using the cosmological constant as the fundamental source of the accelerated behavior, one can develop gravity theories that are equivalent to Λ CDM at the background level yet exhibit distinct and fascinating signatures on perturbation dynamics. Following this notion, we will see if there is a gravity theory with these characteristics that can confront the Λ CDM paradigm.

One of the simplest possibility is introducing an arbitrary function of the Ricci scalar R in the action, which gives the $f(R)$ theory [5–7]. Another two approaches after curvature representations are: the teleparallel gravity in which gravitational force is governed by the torsion T [8–12]. Another possibility employed by Einstein is symmetric teleparallel gravity which attempts to unify field theories. It accounts vanishing curvature and torsion with non-vanishing non-metricity. We will focus at modified gravity based on non-metricity which is a quantity that analyzes how the length of a vector changes when transported.

The symmetric teleparallel gravity or the $f(Q)$ gravity [13–16] is a modified gravity that has recently sparked a lot of interest. When perturbations around the FLRW

background are addressed, the theory shows no strong coupling issues. The $f(Q)$ theory has been studied in a variety of ways, including observational data constraints for various parametrizations of $f(Q)$ [14, 22], cosmography [17], energy conditions [18], black holes [19], bouncing [21, 32], evolution of the growth index in matter perturbations and more [23]. For more works in $f(Q)$ theory, one can check [24–32].

The crossing of the phantom divide line by the dark energy equation of state has two possible cosmic indications [33–38]. One is either the dark energy consists of numerous components, at least one of which is a non-canonical phantom component, or general relativity must be extended to a cosmological scale theory. The current study looks into the cosmic evolution in the exponential [39, 40, 48] and logarithmic [40] $f(Q)$ theories. We investigate the energy density and equation of state parameter in the context of dark energy. The universe with exponential gravity in $f(Q)$ stays in either a non-phantom or a phantom phase without crossing the phantom division line as shown in further study. Moreover, the model behaves like the Λ CDM at high redshifts before deviating to $\omega_{eff} < -1$ or $\omega_{eff} > -1$, respectively depending on the value of a parameter in a model. It also approaches a de-sitter phase asymptotically. Also, the logarithmic $f(Q)$ model behaves in a similar fashion. To realise the crossing of phantom divide line, we use a composite $f(Q)$ model with exponential and logarithmic factor. In this case, ω_{eff} can be seen crossing the phantom division line.

With a negative equation of state, one may deduce the existence of dark energy, but inferring the informa-

* dawrasimran27@gmail.com

† pksahoo@hyderabad.bits-pilani.ac.in

tion about the dynamical feature of ω is difficult. It appears that a higher time derivative of the scale factor is required to obtain the information on the dynamical evolution of ω . The virtue of the statefinder parameters features all kinds of dark energy models. In fact, the statefinder diagnostic has been widely used in a variety of models, including Λ CDM, Chaplygin gas [41, 42], quintessence [43, 44], holographic dark energy models [45, 46], phantom models [47], etc. The spatially flat Λ CDM model corresponds to a fixed point $(r, s) = (1, 0)$. The deviation of a specific dark energy model from this fixed point is a suitable approach to determine the model's departure from the flat Λ CDM.

In addition, we are interested in investigating the stability of cosmological solutions in non-metric models when perturbed by homogeneous perturbations. Typically, homogeneous and isotropic perturbations have been used to determine the stability of several modified gravity theories [54, 55].

The next section introduces $f(Q)$ gravity and derives the field equations. The cosmological formulation of the $f(Q)$ theory is discussed in section III. The cosmic evolution of exponential, logarithmic, and combined $f(Q)$ theories is investigated in section IV. In section V, we discussed the statefinder analysis followed by the linear perturbation analysis in section VI. We also reconstructed the $F(Q)$ gravity using cosmography in section VII. Our conclusions are discussed in section VIII.

II. OVERVIEW OF $f(Q)$ GRAVITY

The action for the non-metricity based $f(Q)$ gravity [15] is given as follows:

$$S = \int \left[\frac{1}{2} f(Q) + L_m \right] \sqrt{-g} d^4x, \quad (1)$$

where L_m represents the matter Lagrangian, g is the determinant of the metric $g_{\mu\nu}$, and $f(Q)$ is an arbitrary function of Q . The basic object in this class of theories is the non-metricity tensor defined as $Q_{\alpha\mu\nu} = \nabla_\alpha g_{\mu\nu}$. Further, the two independent traces and the non-metricity scalar are defined as $Q_\alpha = g^{\mu\nu} Q_{\alpha\mu\nu}$, $\bar{Q}_\alpha = g^{\mu\nu} Q_{\mu\alpha\nu}$ and $Q = -Q_{\alpha\mu\nu} P^{\alpha\mu\nu}$.

The latter expression includes the non-metricity conjugate reads

$$P_{\mu\nu}^\alpha = -\frac{1}{2} L_{\mu\nu}^\alpha + \frac{1}{4} (Q^\alpha - \bar{Q}^\alpha) g_{\mu\nu} - \frac{1}{4} \delta_{(\mu}^\alpha Q_{\nu)}, \quad (2)$$

and the disformation tensor

$$L_{\mu\nu}^\alpha = \frac{1}{2} Q_{\mu\nu}^\alpha - Q_{(\mu\nu)}^\alpha. \quad (3)$$

Let us recall that for $f(Q) = -Q$ [15], the action (1) has been shown to be identical to general relativity (GR) in flat space. As a result, any alteration from GR can be turned into $f(Q)$.

The field equations describing the gravitational interaction in $f(Q)$ gravity is obtained by varying the action with respect to metric tensor

$$\frac{2}{\sqrt{-g}} \nabla_\lambda (\sqrt{-g} f_Q P_{\mu\nu}^\lambda) + \frac{1}{2} g_{\mu\nu} f + f_Q (P_{\mu\lambda\beta} Q_\nu^{\lambda\beta} - 2Q_{\lambda\beta\mu} P_\nu^{\lambda\beta}) = -T_{\mu\nu}, \quad (4)$$

where $f_Q = \frac{df}{dQ}$. Here, $T_{\mu\nu}$ is the stress-energy momentum tensor given by

$$T_{\mu\nu} = \frac{-2}{\sqrt{-g}} \frac{\delta(\sqrt{-g} L_m)}{\delta g^{\mu\nu}}. \quad (5)$$

III. COSMOLOGICAL FORMULATION

We start with the Friedmann-Lemaître-Robertson-Walker (FLRW) metric in a homogeneous and isotropic flat spacetime,

$$ds^2 = -dt^2 + a^2(t)[dx^2 + dy^2 + dz^2], \quad (6)$$

where $a(t)$ is the scale factor of the universe. One can obtain the non-metricity scalar as $Q = 6H^2$, where $H = \frac{\dot{a}}{a}$ is the Hubble parameter. The energy-momentum tensor $T_{\mu\nu}$ for the perfect fluid is given by

$$T_{\mu\nu} = (\rho + p)u_\mu u_\nu + p g_{\mu\nu}, \quad (7)$$

where u_μ is the four-velocity satisfying the condition $u_\mu u^\mu = -1$, ρ and p are the energy density and pressure of a perfect fluid respectively.

On taking $f(Q) = -Q + F(Q)$, the corresponding field equations are

$$H^2 = \frac{1}{3} \rho_m - \frac{F}{6} + \frac{1}{3} Q F_Q, \quad (8)$$

$$(H^2)' = \frac{2p_m + F + Q - 2Q F_Q}{2(2Q F_{QQ} + F_Q - 1)}, \quad (9)$$

where prime denotes a derivative with respect to $\ln a$, $F_Q = \frac{dF(Q)}{dQ}$, $F_{QQ} = \frac{d^2F(Q)}{dQ^2}$. Here, ρ_m , p_m are the energy density and pressure of generic matter, respectively.

By comparing the above modified Friedmann equations with the ordinary ones in general relativity

$$H^2 = \frac{1}{3} (\rho_m + \rho_{eff}), \quad (10)$$

$$(H^2)' = -(\rho_m + p_m + \rho_{eff} + p_{eff}), \quad (11)$$

we get,

$$\rho_{eff} = \frac{1}{2}(-F + 2QF_Q), \quad (12)$$

$$p_{eff} = \frac{F/Q - F_Q + QF_{QQ}}{(2QF_{QQ} + F_Q - 1)(F/Q - 2F_Q)}. \quad (13)$$

Further, using eqns. (12) and (13), the equation of state parameter is obtained as

$$\omega_{eff} = -1 + 4\dot{H} \left(\frac{F_Q + 2QF_{QQ}}{F - 2QF_Q} \right) \quad (14)$$

$$= \frac{F/Q - F_Q + 2QF_{QQ}}{(F/Q - 2F_Q)(2QF_{QQ} + F_Q - 1)}. \quad (15)$$

Considering the non-relativistic matter (i.e., ρ_m and $p_m = 0$), the effective dark energy can be seen satisfying the continuity equation:

$$\rho'_{eff} = \frac{d\rho_{eff}}{d \ln a} = -3(1 + \omega_{eff})\rho_{eff}. \quad (16)$$

IV. COSMOLOGICAL EVOLUTION

We define the dimensionless parameter to study the cosmic evolution of the effective equation of state in $f(Q)$ theory [40, 50]

$$x_H = \frac{H^2}{\bar{m}^2} - a^{-3} = \frac{\rho_{eff}}{\rho_m^0}, \quad (17)$$

where $\bar{m}^2 = \frac{8\pi G \rho_m^0}{3}$. Here $\rho_m^0 = \rho_m(z=0)$ is the present density parameter of non-relativistic matter. From (16), we have the following:

$$x'_H = -3(1 + \omega_{eff})x_H. \quad (18)$$

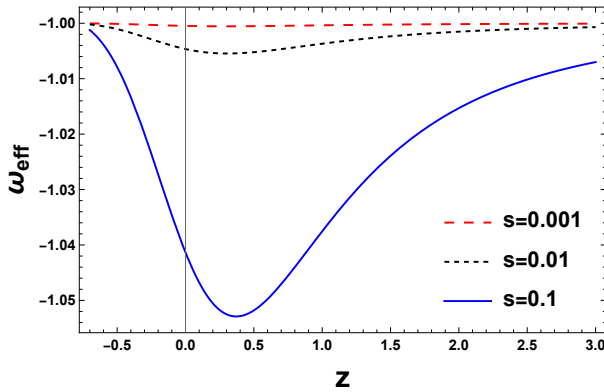
As a result of (17), we obtained $H^2 = \bar{m}^2(x_H + a^{-3})$. It is important to notice that ω_{eff} is a function of Q , whereas Q is a function of H^2 . The relation $a = \frac{1}{1+z}$ is used in subsequent calculations.

A. Model I

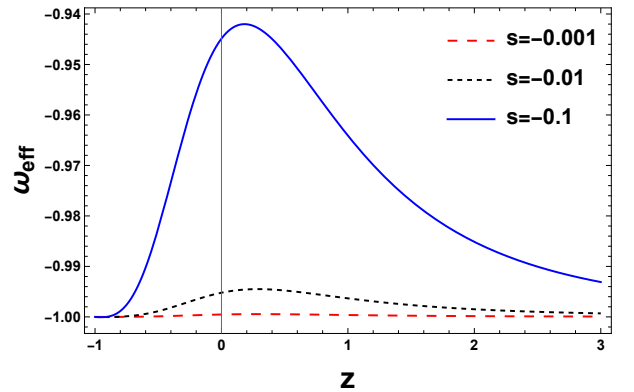
As a first, we consider the exponential $F(Q)$ theory given by [40, 48]

$$F(Q) = \alpha Q(1 - e^{sQ_0/Q}), \quad (19)$$

with $\alpha = \frac{1 - \Omega_m^0}{1 - (1 - 2s)e^s}$, and a constant s . In particular, $s = 0$ corresponds to the usual Friedmann equations as expected. This particular functional form corresponds to the symmetric teleparallel equivalent of general relativity (STEGR). Here, $\Omega_m^0 = \frac{\rho_m^0}{\rho_c^0}$, where ρ_m^0 is the energy density of non-relativistic matter at the present time and $\rho_c^0 = \frac{3H_0^2}{8\pi G}$ is the critical density. Note that the parameters with superscript "0" represents the value at $z = 0$. From the above relations, the dimensionless quantities at $z = 0$ are calculated as: $\frac{\bar{m}^2}{Q_0} = \frac{\Omega_m^0}{6}$ and $x_H(z=0) = \frac{1}{\Omega_m^0} - 1 = 2.17$ for $\Omega_m^0 = 0.315$ [4].



a)



b)

FIG. 1: Evolution of ω_{eff} as a function of redshift z for $|s| = 0.001, 0.01, \text{ and } 0.1$.

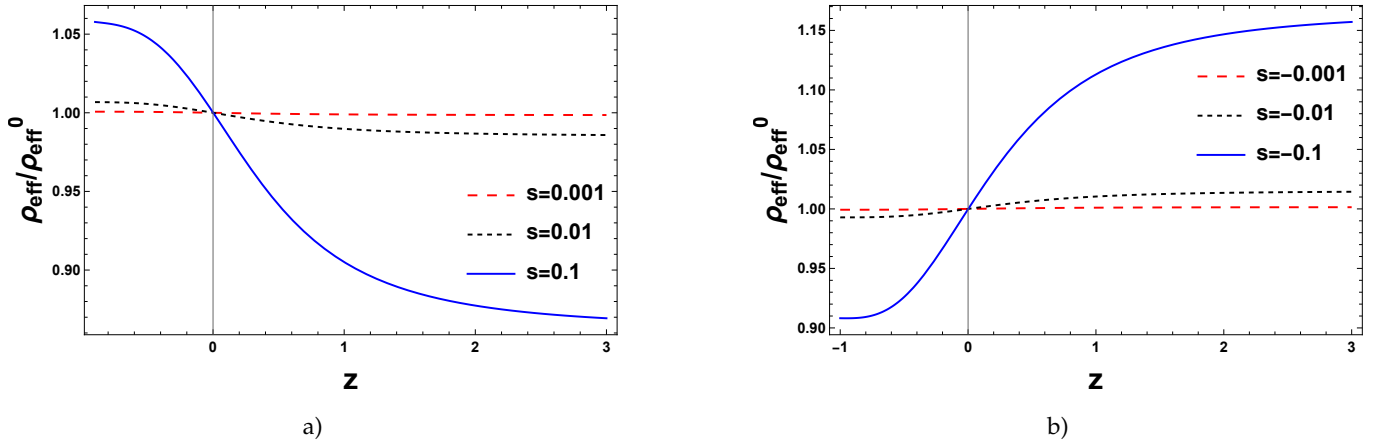


FIG. 2: Evolution of ρ_{eff}/ρ_{eff}^0 as a function of redshift z for $|s| = 0.001, 0.01, \text{ and } 0.1$.

The evolution of the equation of state parameter as functions of redshift for negative and positive values of parameter s is presented numerically in figs. 1a and 1b. It is observed that ω_{eff} does not cross the phantom divide line $\omega_{eff} = -1$ [40, 48]. That is, it lies in phantom phase for $s > 0$ and lies in quintessence phase for $s < 0$. In this work, we choose $|s| = 0.001, 0.01, 0.1$ to see the behavior of exponential $f(Q)$ gravity. It is clear that de-

viation from Λ CDM model for exponential $f(Q)$ gravity is small for smaller s and large for larger s . The present values of ω_{eff}^0 are $-1.0004, -1.0046, -1.0413, -0.999, -0.995, \text{ and } -0.944$ for $s = 0.001, 0.01, 0.1, -0.001, -0.01, \text{ and } -0.1$, respectively [4, 40, 48]. Further figs. 2a and 2b depicts the evolution of ρ_{eff}/ρ_{eff}^0 versus redshift z . It is seen that ρ_{eff}/ρ_{eff}^0 becomes constant in the near future i.e. $z < 0$.

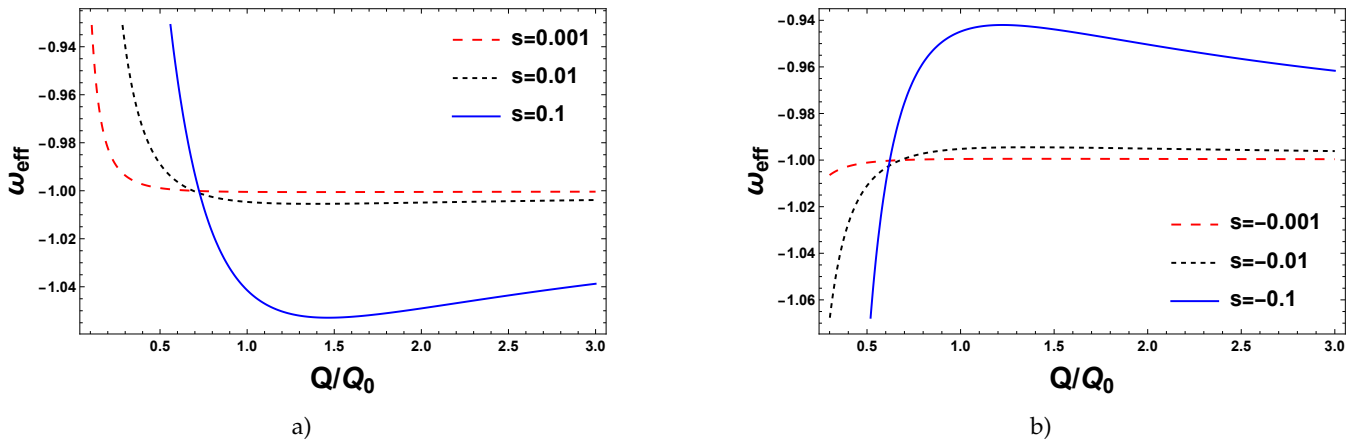


FIG. 3: Evolution of ω_{eff} as a function of Q/Q_0 for $|s| = 0.001, 0.01, \text{ and } 0.1$.

Figs. 3a and 3b illustrates the equation of state ω_{eff} as functions of Q/Q_0 for $s > 0$ and $s < 0$ respectively. It is clear that ω_{eff} versus Q/Q_0 crosses the phantom divide around Q/Q_0 with the large deviation from Λ CDM for $|s| = 0.1$. Furthermore, in cosmological context, the universe reaches the $\omega_{eff} = -1$ with the

crossing point as $Q/Q_0 \simeq 0.686, 0.689, 0.723, 0.684, 0.680, 0.622$ for $s = 0.001, 0.01, 0.1, -0.001, -0.01, \text{ and } -0.1$, respectively .

Crossing of the phantom divide line:

Note that from eq. (14), ω_{eff} crosses -1 if $4\dot{H} \left(\frac{F_Q + 2QF_{QQ}}{F - 2QF_Q} \right)$ changes its sign. According to eq. (19), we have

$$F_Q = \alpha \left(1 - e^{sQ_0/Q} + \frac{sQ_0}{Q} e^{sQ_0/Q} \right), \quad (20)$$

and

$$F_{QQ} = -\alpha \left(\frac{sQ_0}{Q} \right)^2 \frac{1}{Q} e^{sQ_0/Q}. \quad (21)$$

For the investigation, if we concentrate on $0 < s \ll 1$ and $A = \frac{sQ_0}{Q} \ll 1$. So, we obtained the following using approximation to second order:

$$\frac{F}{Q} - 2F_Q \approx -\alpha A \left(1 + \frac{3A}{2} \right), \quad (22)$$

and

$$F_Q + 2QF_{QQ} \approx -\frac{3\alpha A^2}{2}. \quad (23)$$

Here, both the equations have same sign implies that $\frac{F_Q + 2QF_{QQ}}{F/Q - 2F_Q}$ does not change its sign. Henceforth, ω_{eff} do not cross the phantom divide line.

In figs. 4a, 4b we show the fractional densities of effective dark energy and the non-relativistic matter as functions of redshift z , i.e. $(\Omega_{eff} = \frac{\rho_{eff}}{\rho_c}, \Omega_m = \frac{\rho_m}{\rho_c})$. Furthermore, the cosmological evolution of Ω_{eff} and Ω_m for other values of model parameter $|s| = 0.01$ and 0.001 is similar to $|s| = 0.1$. The intersection of Ω_{eff} and Ω_m is the crossover point z_{eff} at which $\Omega_{eff} = \Omega_m$. The universe reaches the matter-dominated stage as z decreases. When $z < z_{eff}$, dark energy eventually overcomes matter. The present values for the parameters are obtained as $\Omega_{eff}^{(0)} = 0.68$, $\Omega_m^{(0)} = 0.314$, and $z_{eff} = 0.28$ and 0.31 , respectively.

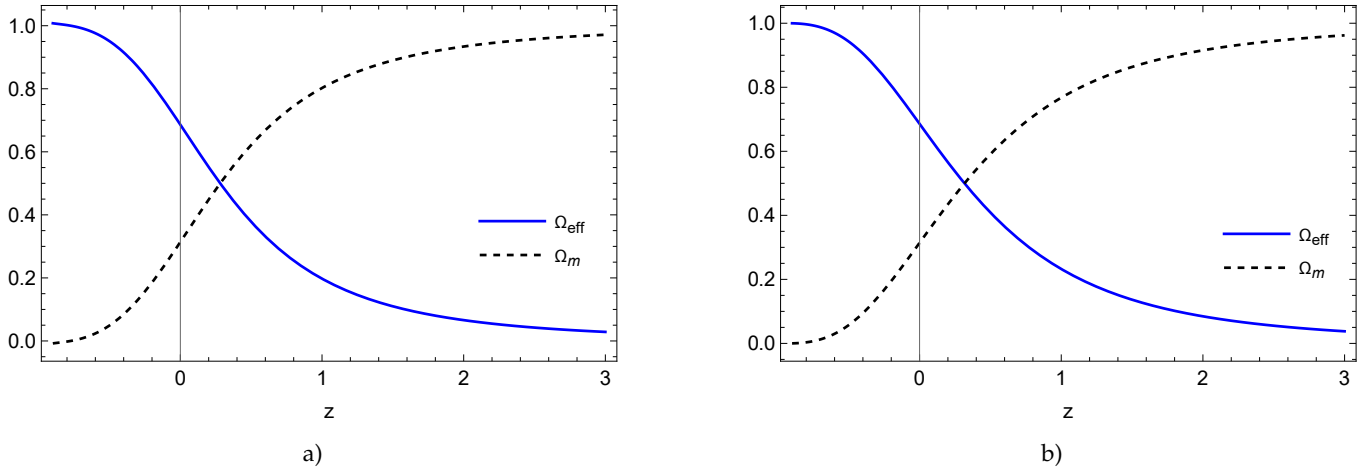


FIG. 4: Evolution of Ω_{eff} and Ω_m as a function of z for $|s| = 0.1$ respectively.

B. Model II

Here, we consider another motivated logarithmic $F(Q)$ model given by

$$F(Q) = \gamma Q_0 \left(\frac{kQ_0}{Q} \right)^{-\frac{1}{2}} \ln \left(\frac{kQ_0}{Q} \right), \quad (24)$$

where $\gamma = \frac{\Omega_m^0 - 1}{2k^{-1/2}}$ and a constant k . It is seen that the model contains only one parameter k for the given Ω_m^0 .

Fig. 5a and 5b describes the behavior of ω_{eff} as func-

tions of redshift z and Q/Q_0 respectively for the parameter $k = 1$. It is observed that ω_{eff} lies in a quintessence region and do not cross the phantom divide line. The present value of ω_{eff}^0 is -0.760 [49]. After simplifying (14) for this model, we get

$$\omega_{eff} = -\frac{1}{2 - (1 - \Omega_m^0) \left(\frac{Q_0}{Q} \right)^2}, \quad (25)$$

which implies that ω_{eff} does not depend on the parameter k and hence similarly cannot cross the phantom

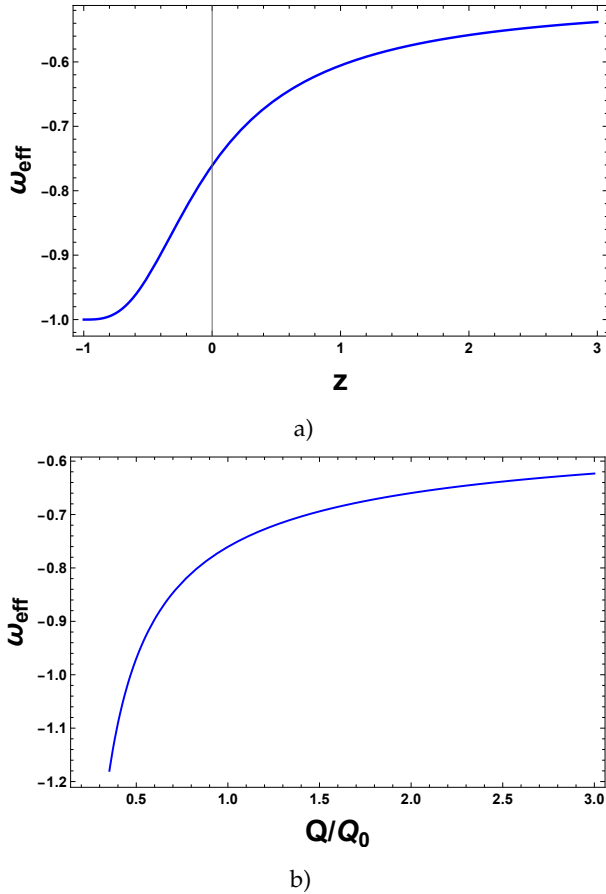


FIG. 5: Evolution of ω_{eff} as a function of redshift z and Q/Q_0 , respectively for $k = 1$.

divide line. Here, ω_{eff} crosses -1 at $Q/Q_0 \simeq 0.4692$.

In fig. 6, the cosmological evolution of Ω_{eff} and Ω_m for the parameter $k = 1$ is presented. Furthermore, the intersection of Ω_{eff} and Ω_m is the crossover point z_{eff}

Fig. 7a indicates the behavior of ω_{eff} versus redshift z for $v = 0.5$, $v = 0.8$ and $v = 1$. We have considered the values of model parameters constrained in ref. [40, 48]. It is clear that ω_{eff} shows a transition from a non-phantom phase to a phantom phase with the present values as -0.927 , -1.068 , and -1.133 [34], respectively. It is noted that the universe crosses the phantom divide line and may approach to $\omega_{eff} = -1$ in the near future.

We can also see in fig. 7b that ω_{eff} crosses -1 at $Q/Q_0 = 0.764$ and 0.806 for $v = 0.8$ and $v = 1$, respectively. Furthermore, the evolution of ρ_{eff}/ρ_{eff}^0 is presented in fig. 7c which shows that effective density becomes dom-

inant in near future. at which $\Omega_{eff} = \Omega_m$. The universe reaches the matter-dominated stage as z decreases. When $z < z_{eff}$, dark energy eventually overcomes matter. The present values for the parameters are obtained as $\Omega_{eff}^{(0)} = 0.68$, $\Omega_m^{(0)} = 0.314$, and $z_{eff} \approx 0.4$.

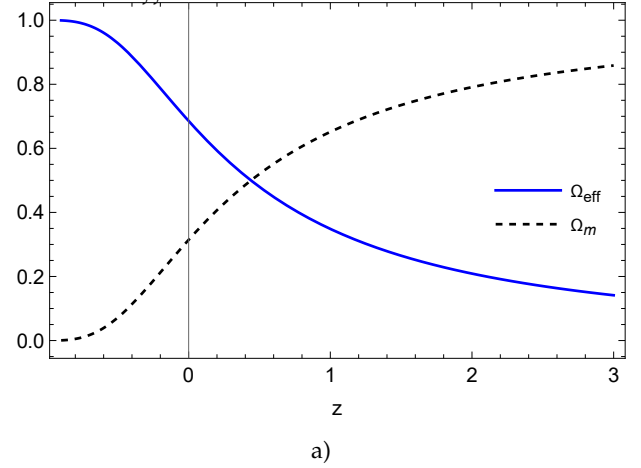


FIG. 6: Evolution of Ω_{eff} and Ω_m as functions of redshift z for $k = 1$.

C. Model III

In this subsection, we consider the combination of exponential and logarithm $F(Q)$ theory to study the cosmological evolution and crossing of phantom divide line. The functional form read as

$$F(Q) = \beta \left[Q_0 \left(\frac{vQ_0}{Q} \right)^{-1/2} \ln \left(\frac{vQ_0}{Q} \right) - Q(1 - e^{vQ_0/Q}) \right], \quad (26)$$

with $\beta = \frac{\Omega_m^0 - 1}{2v^{-1/2} + (1 - e^{v(1-2v)})}$, where v is a constant.

inant in near future.

Crossing of the phantom divide line:

Note that from eq. (14), ω_{eff} crosses -1 if $4\dot{H} \left(\frac{F_Q + 2QF_{QQ}}{F - 2QF_Q} \right)$ changes its sign.

For the investigation, if we concentrate on $\frac{vQ_0}{Q} \ll 1$, we obtained the following using approximation to second order:

$$\frac{F}{Q} - 2F_Q \approx \beta \sqrt{\frac{Q_0 v}{Q}} \left[\frac{2}{v} + \sqrt{\frac{Q_0 v}{Q}} \left(1 + \frac{3}{2} \frac{Q_0 v}{Q} \right) \right], \quad (27)$$

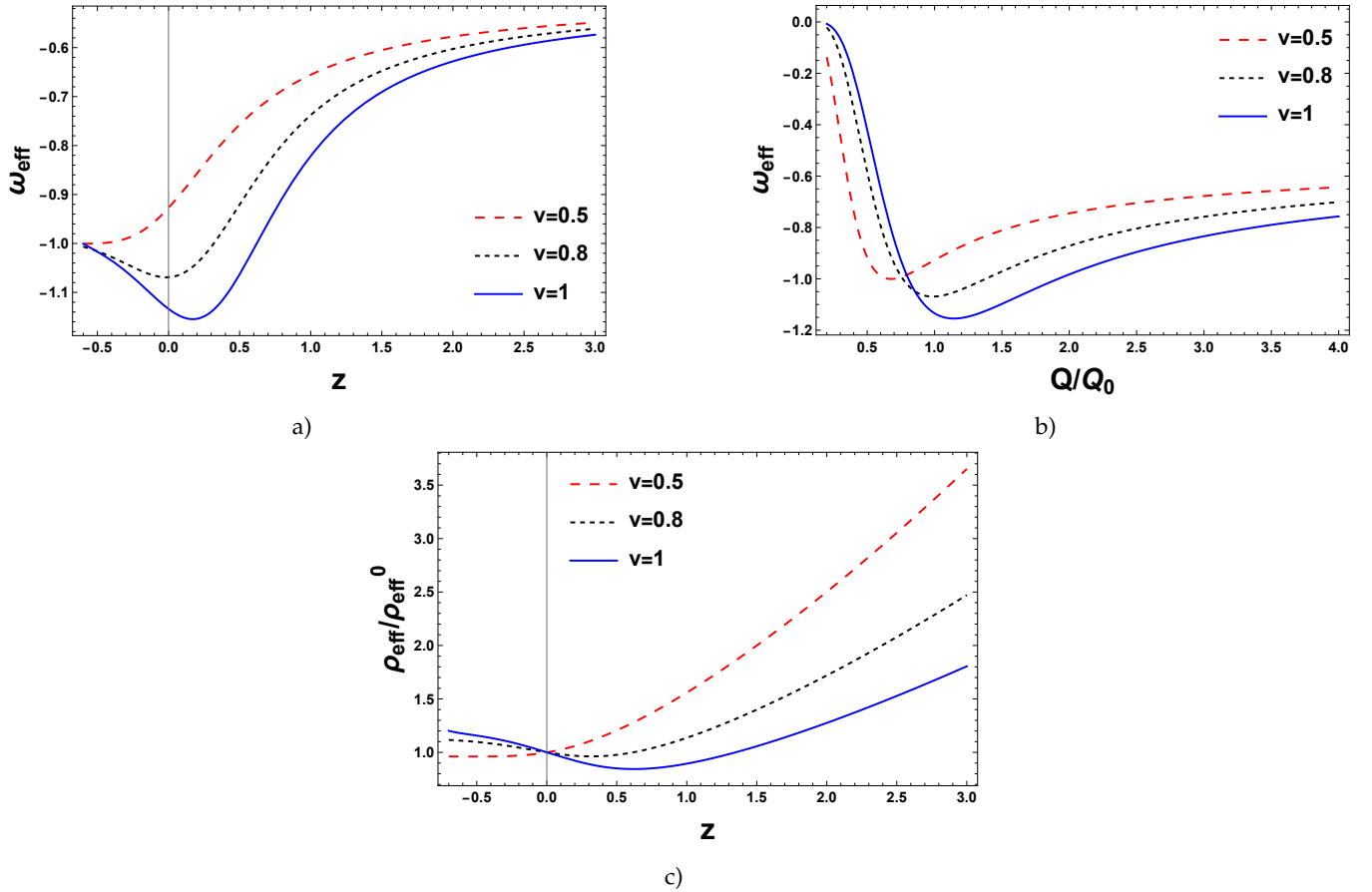


FIG. 7: Evolution of ω_{eff} as a function of redshift z and Q/Q_0 for $v = 0.5, 0.8$ and 1 . The subplot (c) shows ρ_{eff}/ρ_{eff}^0 as a function of redshift z for $v = 0.5, 0.8$ and 1 .

and

$$F_Q + 2QF_{QQ} \approx -\beta \sqrt{\frac{Q_0 v}{Q}} \left[\frac{1}{v} - \frac{3}{2} \left(\frac{Q_0 v}{Q} \right)^{3/2} \right]. \quad (28)$$

Here, the equations have different sign implies that $\frac{F_Q + 2QF_{QQ}}{F/Q - 2F_Q}$ does change its sign for the critical point $\frac{Q_0 v}{Q} = \left(\frac{2}{3v} \right)^{2/3}$. Henceforth, ω_{eff} crosses the phantom divide line in the combined $f(Q)$ model.

Figs. 8 shows the evolution of Ω_{eff} and Ω_m for value of parameter $v = 0.5$. The crossover point z_{eff} for this model is $z_{eff} \approx 0.34, 0.27, 0.25$, respectively for $v = 0.5, v = 0.8$, and $v = 1$. The universe reaches the matter-dominated stage as z decreases. When $z < z_{eff}$, dark energy eventually overcomes matter. The present values for the parameters are obtained as $\Omega_{eff}^{(0)} \approx 0.68, \Omega_m^{(0)} \approx 0.314$ for all the three values of v .

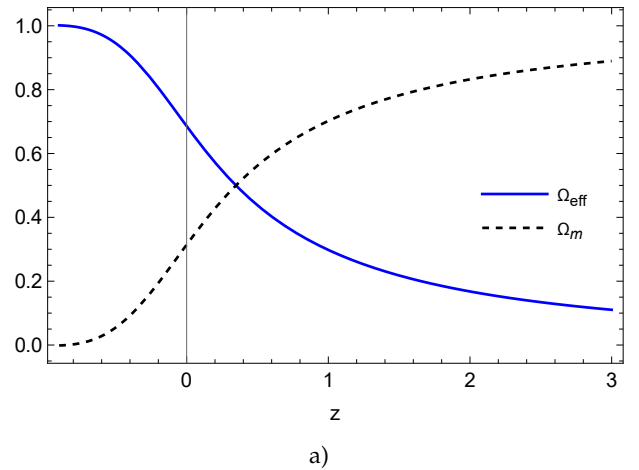


FIG. 8: Evolution of Ω_{eff} and Ω_m as functions of redshift z for $v = 0.5$.

V. STATEFINDER DIAGNOSTICS

A new set of geometrical diagnostics for dark energy with the goal of distinguishing and classifying different dark energy models is proposed by Sahni et al. [43] and Alam et al. [41]. The scale factor $a(t)$ and its derivatives up to the third order are used to construct the statefinder diagnostics. Since the statefinder pair $\{r, s\}$ has a geometrical nature, the statefinder parameters are more universal parameters to analyze dark energy models. The diagnostic pair is defined as follows:

$$r = \frac{\ddot{a}}{aH^3},$$

$$s = \frac{r - 1}{3(q - \frac{1}{2})}.$$

Here, $q = -\frac{a\ddot{a}}{\dot{a}^2}$. For more on statefinder analysis, one can check References [51–53]. We plot the trajectories in $\{s, r\}$ and $\{q, r\}$ plane for all the three models. It is clear from the figs. 9a, 9b, and 9c that the dark energy models always approaches to Λ CDM model, i.e. $(s, r) = (0, 1)$ in the late time evolution. It is interesting to note that the trajectory in the case of model III passes through the Λ CDM point but may not approach to the Λ CDM at late times.

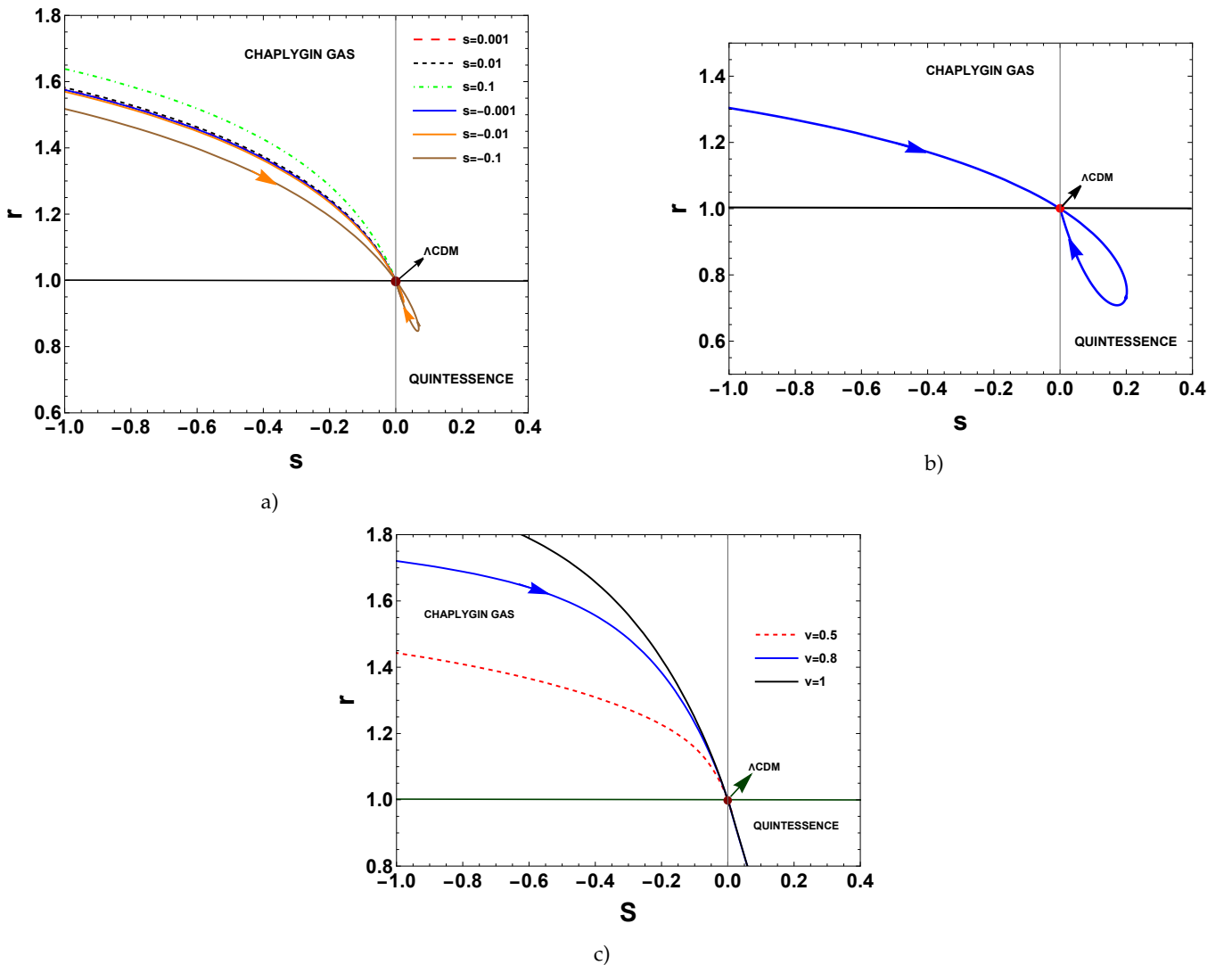


FIG. 9: Trajectories of $s - r$ plane for model I, model II and model II, respectively.

Fig. 10a, 10b, and 10c plot the trajectories in $q - r$ plane for model I, model II and Model III. The dS model

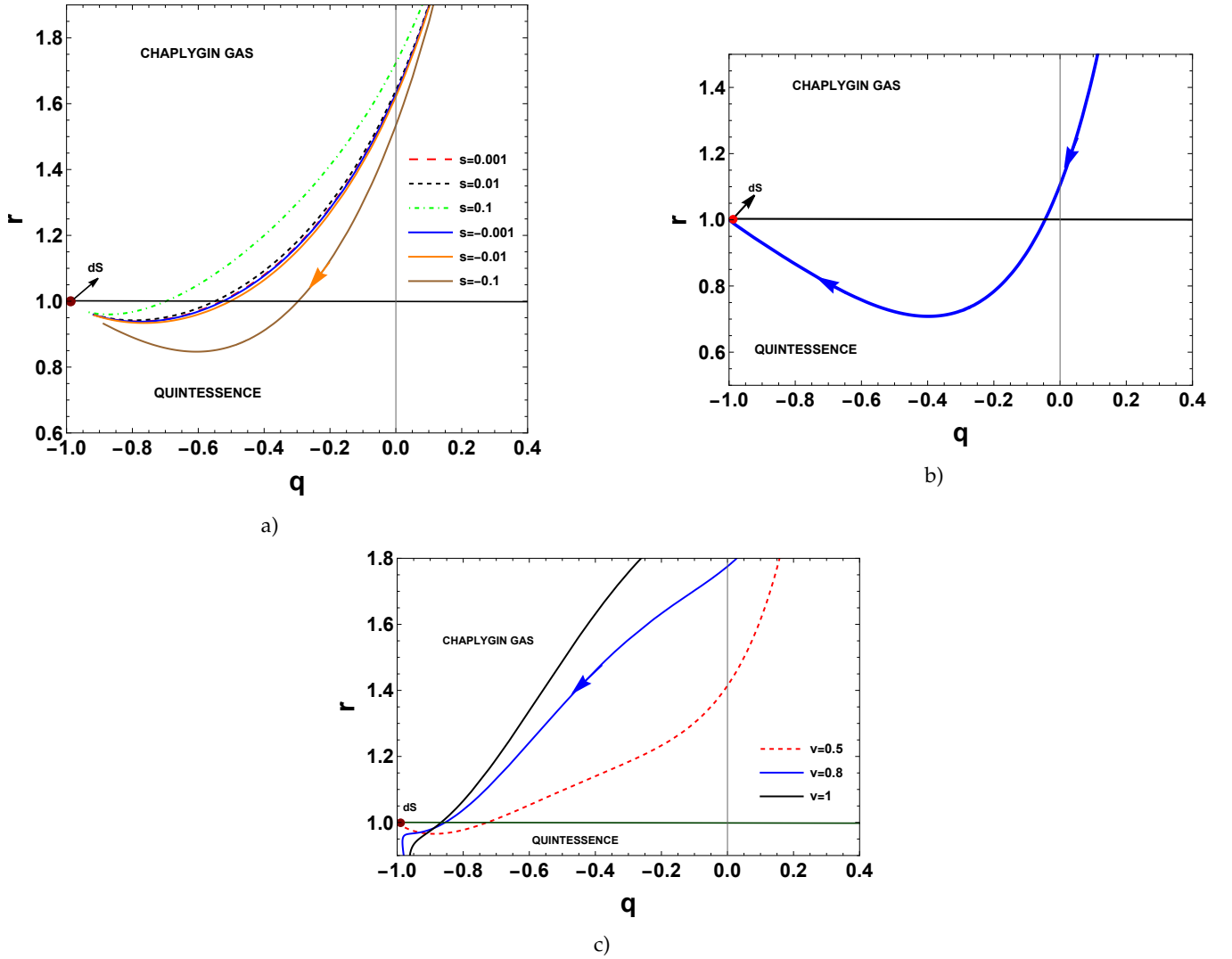


FIG. 10: Trajectories of $q - r$ plane for model I, model II and model II, respectively.

(steady state) have been shown by the point $(q, r) = (-1, 1)$. The recent phase transition is satisfactorily explained by the signature flip of the deceleration parameter q from positive to negative. One can observe that,

for different values of respective parameters for model I and model II, the dark energy model approaches the dS point as Chaplygin gas, Λ CDM and quintessence at late time evolution. Furthermore, in case of model III, the trajectories deviates from dS model at late times.

VI. LINEAR PERTURBATIONS ANALYSIS

In the present section, we investigate the stability of the cosmological models considered under the homogeneous linear perturbations. One can define the first order perturbation for the Hubble and density parameter as [54–56]

$$\widetilde{H}(t) = H(t)(1 + \delta) \quad (29)$$

$$\widetilde{\rho}(t) = \rho(t)(1 + \delta_m). \quad (30)$$

Here, $\widetilde{H}(t)$, and $\widetilde{\rho}(t)$ represents the perturbed Hubble and density parameter, δ and δ_m are the perturbation terms, respectively. Now eqns. (8) and (9) can be simplified to

$$\frac{\dot{f}}{2} - Qf_Q = \rho \quad (31)$$

$$(f_Q + 2Qf_{QQ}) \dot{H} = \frac{1}{2} (\rho + p). \quad (32)$$

which are satisfied by the perturbed quantities with the continuity equation. We can obtain the perturbed f and f_Q as $\delta f = f_Q \delta Q$ and $\delta f_Q = f_{QQ} \delta Q$ with $\delta Q = 12H\delta H$. Now, using the continuity equation and (31), we get the following equations:

$$Q(f_Q + 2Qf_{QQ}) \delta = -\rho \delta_m, \quad (33)$$

$$\dot{\delta}_m + 3H(1 + \omega)\delta = 0. \quad (34)$$

Solving the above equations for δ and δ_m , we have

$$\dot{\delta}_m - \frac{3H(1 + \omega)\rho}{Q(f_Q + 2Qf_{QQ})} \delta_m = 0. \quad (35)$$

Simplifying the above equation using eqn. (32), the solution read as

$$\delta_m = \delta_{m_0} H \quad (36)$$

$$\delta = \delta_0 \frac{\dot{H}}{H} = \delta_0 (1 + z) \frac{dH}{dz}, \quad (37)$$

where δ_{m_0} is constant. Also $\delta_0 = -\frac{\delta_{m_0}}{3(1+\omega)}$. We present the behavior of perturbation terms δ_m and δ with respect to redshift z in figs. 11a, 11b, and 11c for model I, model II and model III, respectively. It is clear that δ_m and δ decay rapidly at late times and depicts the stability of our considered models.

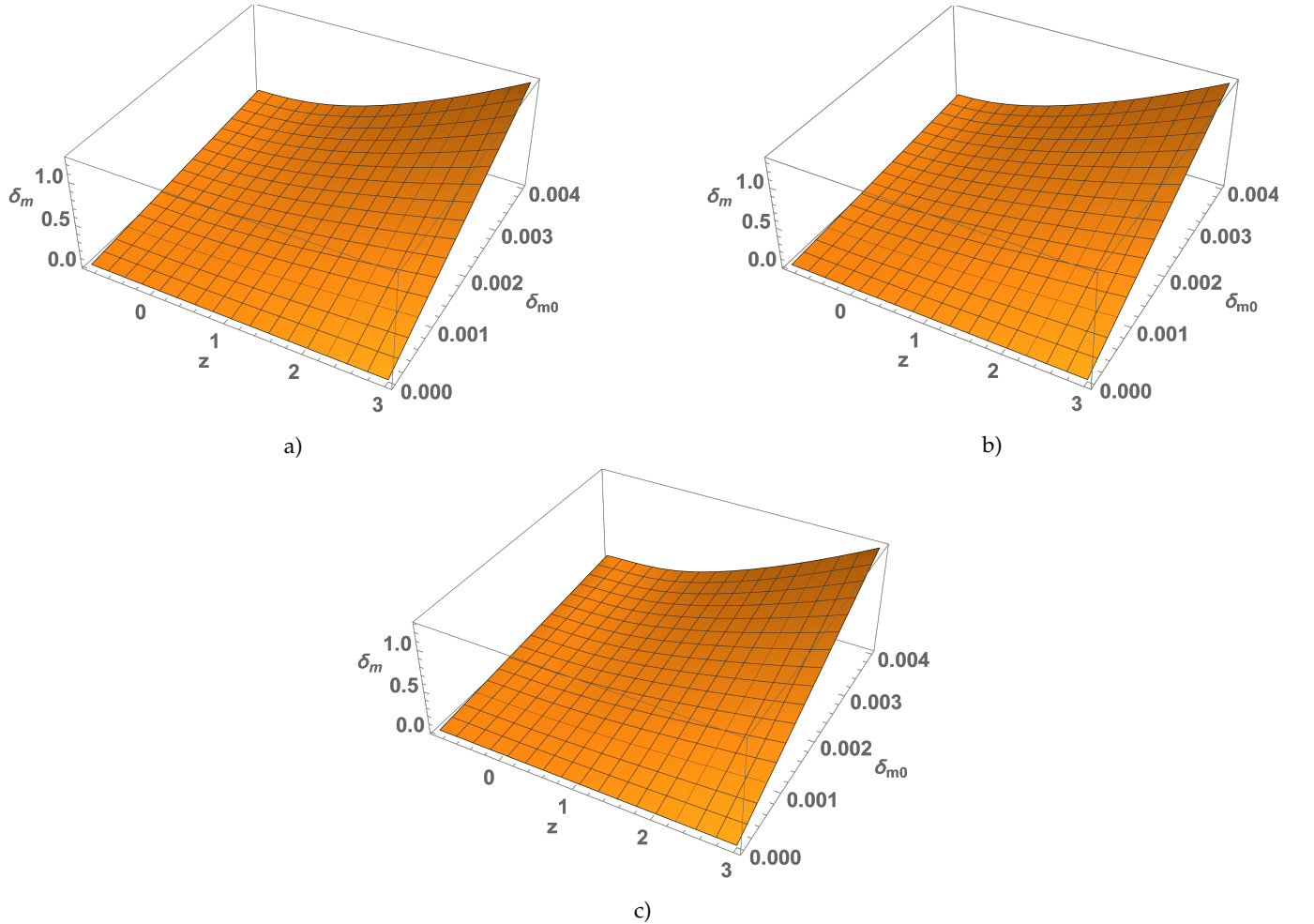


FIG. 11: Evolution of δ_m for model I, model II and model III with $0 < \delta_{m_0} < 0.004$, respectively.

It is seen that the evolution of δ_m is similar for all the model parameters. The evolution of δ is presented in figs. 12a, 12b, and 12c for $s = 0.1$, $k = 1$, and $v = 0.8$.

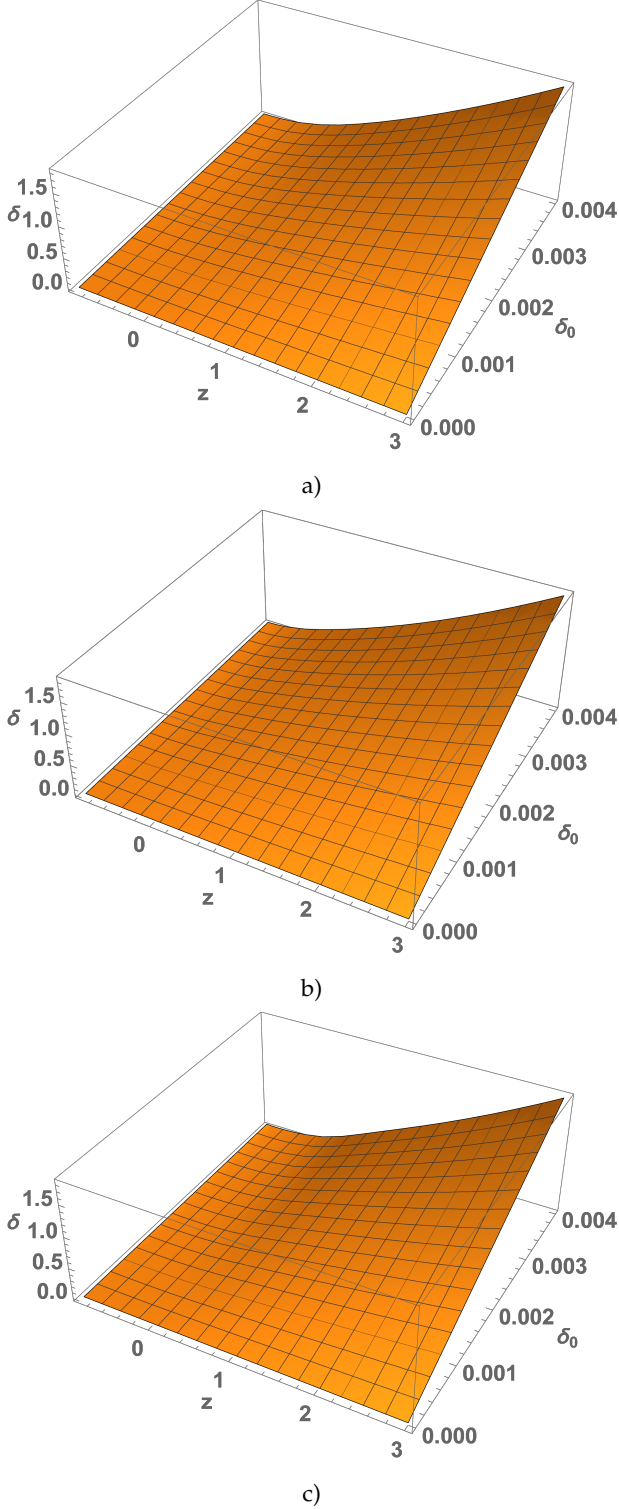


FIG. 12: Evolution of δ for model I, model II and model III with $0 < \delta_0 < 0.004$, respectively.

VII. RECONSTRUCTION OF $F(Q)$

The cosmographic technique allows to explore the dynamics of the universe using kinematic quantities that are independent of the background cosmology. Thus, the late-time expansion history of the universe can be examined to the cosmological principle in order to obtain information on the dark energy attributes and the nature of gravity. Pad'e approximations [58] are one of the most dependable cosmographic strategies for ensuring steady behavior at high redshifts. The corresponding Hubble expansion is obtained as [57]

$$H(z) = H_0 \frac{M(z; q_0, j_0)}{N(z; q_0, j_0)}, \quad (38)$$

where

$$\begin{aligned} M(z; q_0, j_0) &= 2(1+z)^2(3+z+j_0z-3q_0^2z-q_0(3+z))^2 \\ N(z; q_0, j_0) &= 18+6(5+2j_0)z+(14+7j_0+2j_0^2)z^2+9q_0^4z^2 \\ &\quad +18q_0^3z(1+z)-2q_0(6+5z)(3+(4+j_0)z) \\ &\quad +q^2(18+30z+(17-9j_0)z^2). \end{aligned}$$

We use the values of cosmographic parameters as $H_0 = 69$, $q_0 = -0.73$ and $j_0 = 2.84$ [59]. The term F_Q can be written in terms of Hubble parameter as a function of redshift z , i.e. $F_Q = \frac{F'(z)}{12H(z)H'(z)}$, where $F'(z)$ is the derivative of F with respect to z . Hence, we can write eqn. (8) as

$$\frac{H(z)F'(z)}{H'(z)} - F(z) + 6H_0^2\Omega_{m_0}(1+z)^3 - 6H^2 = 0. \quad (39)$$

According to the analysis in [57], we use the initial condition $F_Q(z=0) = 1$ leading to $F_0 = 6H_0^2(1 + \Omega_{m_0})$. Solving numerically gives the similar trajectory in fig. 13 mentioned in [57] as $F(Q) = \zeta + \sigma Q^n$.

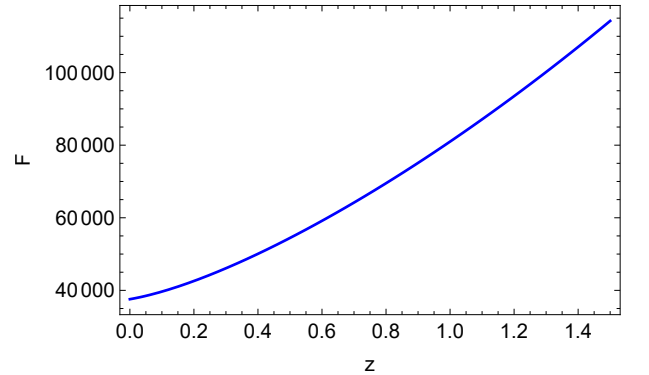


FIG. 13: Evolution of F versus z .

To see if the phantom divide line crosses for $F(Q) = \zeta + \sigma Q^n$, we look at whether $4\dot{H} \left(\frac{F_Q + 2QF_{QQ}}{F - 2QF_Q} \right)$ changes its

sign.

$$\frac{F}{Q} - 2F_Q = \frac{\zeta + \sigma Q^n(1 - 2n)}{Q}$$

$$F_Q + 2QF_{QQ} = -n(1 - 2n)\sigma Q^{n-1}.$$

According to the trajectory of F , we can assure that $\zeta > 0$ and $\sigma > 0$. Furthermore, the equations above have different signs for any value of n . This depicts that ω_{eff} may cross the phantom divide line in the obtained $F(Q)$ model.

VIII. CONCLUSION

The newly proposed extended symmetric teleparallel or the $f(Q)$ gravity theory is an exciting extension of Einstein's new general relativity, employing a non-metricity Q rather than curvature. Recently, there has been renewed interest in Einstein's new equivalent theories for obtaining cosmic acceleration. We may discover that Einstein predicted the cosmic acceleration not necessarily through the cosmological constant but also through the equivalent representation of general relativity.

We investigated the cosmic evolution in the exponential and logarithmic $F(Q)$ theories. In the exponential $F(Q)$ model, the universe is observed to be in the non-phantom regime without crossing the phantom divide line. Similarly, the logarithmic $F(Q)$ theory with one model parameter does not permit phantom divide crossing.

Furthermore, the crossing of the phantom division line from a non-phantom phase to a phantom phase is a re-

markable characteristic of the combination of exponential and logarithmic $F(Q)$ model. It is also worth noting that the phantom divide crossing is compatible with the observations. In section V, we discussed the statefinder diagnostics to differentiate various dark energy models. It is observed that the dark energy models always approaches to Λ CDM model, i.e. $(s, r) = (0.1)$ in the late time evolution. Also, it is noted that the trajectory in the case of model III passes through the Λ CDM point but may not approach to the Λ CDM at late times. There is a large deviation from Λ CDM point in case of the combined $F(Q)$ model.

Further, in section VI, the perturbed equations are solved analytically and depends on the Hubble parameter. It is either decaying to zero at late times or being identically zero for the Hubble perturbation. The matter perturbation, on the other hand, likewise decays to zero. As a result, this solution can be regarded as stable with respect to small perturbations and hence implying the stability of $F(Q)$ models. We also used the numerical inversion approach to rebuild the $F(Q)$ using the relation $Q = 6H^2$. We discovered that the function $F(Q) = \zeta + \sigma Q^n$ provides the best analytical fit and may cross the phantom divide line at late times. As a result, the work demonstrates that the non-metric theories can be used to drive the cosmic acceleration.

ACKNOWLEDGEMENTS

SA acknowledges CSIR, New Delhi, India for JRF. PKS acknowledges CSIR, New Delhi, India for financial support to carry out the Research project [No.03(1454)/19/EMR-II Dt.02/08/2019].

-
- [1] A.G. Riess et al., *Astron. J.*, **116**, 1009 (1998).
 - [2] S. Perlmutter et al., *Astrophys. J.*, **517**, 565 (1999).
 - [3] P.A.R. Ade et al., *Astron. Astrophys.*, **594**, A13 (2016).
 - [4] N. Aghanim et al., *A&A*, **641**, A6 (2020).
 - [5] H.A. Buchdahl, *Month. Not. R. Astron. Soc.*, **150**, 1 (1970).
 - [6] S. Capozziello, V. F. Cardone, V. Salzano, *Phys. Rev. D*, **78**, 063504 (2008).
 - [7] A. de la Cruz-Dombriz, A. Dobado, *Phys. Rev. D*, **74**, 087501 (2006).
 - [8] S. Capozziello et al., *Phys. Rev. D*, **84**, 043527 (2011).
 - [9] Di Liu, M. J. Reboucas, *Phys. Rev. D*, **86**, 083515 (2012).
 - [10] L. Iorio, E. N. Saridakis, *Month. Not. R. Astron. Soc.*, **427**, 1555 (2012).
 - [11] Deng Wang, David Mota, *Phys. Rev. D*, **102**, 063530 (2020).
 - [12] R. C. Nunes, S. Pan, E. N. Saridakis, *JCAP*, **08**, 011 (2016).
 - [13] J.M. Nester, H.-J. Yo, *Chin. J. Phys.*, **37**, 113 (1999).
 - [14] R. Lazkoz et al., *Phys. Rev. D*, **100**, 104027 (2019).
 - [15] J. Beltran Jimenez, L. Heisenberg, T. Koivisto, *Phys. Rev. D*, **98**, 044048 (2018).
 - [16] J. Beltran Jimenez et al., *Phys. Rev. D*, **101**, 103507 (2020).
 - [17] S. Mandal, D. Wang, P.K. Sahoo, *Phys. Rev. D*, **102**, 124029 (2020).
 - [18] S. Mandal, P.K. Sahoo, J.R.L. Santos, *Phys. Rev. D*, **102**, 024057 (2020).
 - [19] F. D'Ambrosio et al., *Phys. Rev. D*, **105**, 024042 (2022).
 - [20] F. Bajardi, D. Vernieri, S. Capozziello, *Eur. Phys. J. Plus*, **135**, 912 (2020).
 - [21] S. Mandal et al., *Eur. Phys. J. Plus*, **136**, 760 (2021).
 - [22] I. Ayuso, R. Lazkoz, V. Salzano, *Phys. Rev. D*, **103**, 063505 (2021).
 - [23] W. Khylllep, A. Paliathanasis, Jibitesh Dutta, *Phys. Rev. D*, **103**, 103521 (2021).

- [24] I.S. Albuquerque, N. Frusciante, *Phys. Dark Univ.*, **35**, 100980 (2022).
- [25] F. Esposito et al., *Phys. Rev. D*, **105**, 084061 (2022).
- [26] L. Atayde, N. Frusciante, *Phys. Rev. D*, **104**, 064052 (2021).
- [27] D. Zhao, *Eur. Phys. J. C*, **82**, 303 (2022).
- [28] N. Frusciante, *Phys. Rev. D*, **103**, 044021 (2021).
- [29] N. Dimakis, A. Paliathanasis, T. Christodoulakis, *Class. Quantum Gravit.*, **38**, 225003 (2021).
- [30] B.J. Barros et al., *Phys. Dark Univ.*, **30**, 100616 (2020).
- [31] T. Harko et al., *Phys. Rev. D*, **98**, 084043 (2018).
- [32] F. Bajardi, D. Vernieri, S. Capozziello, *Eur. Phys. J. C*, **135**, 912 (2020).
- [33] P. S. Apostolopoulos, N. Tetradis, *Phys. Rev. D*, **74**, 064021 (2006).
- [34] P. Wu, H. Yu, *Eur. Phys. J. C*, **71**, 1552 (2011).
- [35] K. Nozari, M. Pourghasemi, *JCAP*, **10**, 044 (2008).
- [36] K. Bamba, C.-Q. Geng, C.-C. Lee, *JCAP*, **11**, 001 (2010).
- [37] J. Lu, X. Zhao, G. Chee, *Eur. Phys. J. C*, **79**, 530 (2019).
- [38] S. Karimzadeh, R. Shojaei, *Adv. High Energy Phys.*, **2019**, 4026856 (2019).
- [39] L. Yang et al., *Phys. Rev. D*, **82**, 103515 (2010).
- [40] K. Bamba et al., *JCAP*, **01**, 021 (2011).
- [41] U. Alam et al., *Mon. Not. Roy. Astron. Soc.*, **344**, 1057-1074 (2003).
- [42] V. Gorini, A. Kamenshchik, U. Moschella, *Phys. Rev. D*, **67**, 063509 (2003).
- [43] V. Sahni et al., *Jetp Lett.*, **77**, 201-206 (2003).
- [44] X. Zhang, *Phys. Lett. B*, **611**, 1 (2005).
- [45] J. Zhang, X. Zhang, H. Liu, *Phys. Lett. B*, **659**, 26-33 (2008).
- [46] M.R. Setare, *Phys. Lett. B*, **653**, 116-121 (2007).
- [47] B. Chang et al., *JCAP*, **01**, 016 (2007).
- [48] Eric V. Linder, *Phys. Rev. D*, **81**, 127301 (2010).
- [49] S. Mandal, P.K. Sahoo, *Phys. Lett. B*, **823**, 136786 (2021).
- [50] W. Hu, I. Sawicki, *Phys. Rev. D*, **76**, 064004 (2007).
- [51] R. Solanki et al., *Phys. Dark Univ.*, **32**, 100820 (2021).
- [52] S.K.J. Pacif, S. Arora, P.K. Sahoo, *Phys. Dark Univ.*, **32**, 100804 (2021).
- [53] H. Shabani, *Int. J. Mod. Phys. D*, **26**, 1750120 (2017).
- [54] G. Farrugia, J. L. Said, *Phys. Rev. D*, **94**, 124054 (2016).
- [55] A. de la C-Dombriz, D. S-Gomez, *Class. Quantum Grav.*, **29**, 245014 (2012).
- [56] F. K. Anagnostopoulos, S. Basilakos, E. N. Saridakis, *Phys. Lett. B*, **822**, 136634 (2021).
- [57] S. Capozziello, R. D'Agostino, *Arxiv*: 2204.01015 (2022).
- [58] C. Gruber, O. Luongo, *Phys. Rev. D*, **89**, 103506 (2014).
- [59] S. Capozziello, R. D'Agostino, O. Luongo, *Mon. Not. Roy. Astron. Soc.*, **494**, 2576 (2020).